*Science & Technology Development Journal – Engineering and Technology, 4(SI2):SI57-SI67*

Open Access Full Text Article

*Research article*

# Analysis the influence of threaded pin profiles in friction stir welding by numerical simulation

**Do Huynh Nhu[1,2], Vu Cong Hoa[1,2,*]**

Use your smartphone to scan this QR code and download this article

**ABSTRACT**

Currently, the welding industry has made significant contributions in most production fields to meet the needs of people's lives. However, traditional welding methods have disadvantages such as: a large amount of energy consumption, production of many toxic gases that are harmful to the environment and the health of workers. Therefore, the friction stir welding method was introduced from the research of scientists to overcome the above disadvantages. Besides that, it is suitable for welding aluminum alloys and non-ferrous metals with low melting point. This green welding technology has been continuously researched to improve weld quality through two main research models: experiment models and numerical simulation models. Experimental results provides the basic mechanical properties of the materials at the weld and the process optimization parameters. It will be the basis to establish a numerical simulation model closest to reality, based on mathematical models and working principles, thereby helping to predict weld quality through prediction of formation defects, temperature distribution with changes in welding process parameters such as time, velocity, material or welding pin profile. In this study, the influence of threaded pin profiles on weld quality of alloy aluminum 7075 -T6 during friction stir welding was investigated by numerical simulation model through ABAQUS software to recommend a new pin profile bringing an efficient welding process. To increase the reliability of this research approach, the numerical simulation results of the temperature distribution are compared with the experimental results obtained from a foreign scientific paper with an average error of 14%. Threaded pin profiles are designed in combination with three cross-sections having different opening angles named TF0, TF30, TF60 and TF90. Coupled Eulerian-Lagrangian formulation is applied for this model where the welding tool is Lagrangian domain and workpiece is Eulerian domain. Because material deformation in friction stir welding process is large and related to temperature, the elastic-plastic Johnson-Cook model is used for workpiece. Results of this research shows a new pin profile named TF60 which it gives the best weld quality of the four configurations of the pin tool examined in this study through evaluating temperature distribution and predicting weld defect formation. [1–22]

**Key words:** Friction stir welding, threaded pin profile, Coupled Eulerian-Lagrangian, Johnson – Cook model, welding simulation

[1]*Department of Engineering Mechanics, Faculty of Applied Sciences, Ho Chi Minh City University of Technology, 268 Ly Thuong Kiet Street, District 10, Ho Chi Minh City, Vietnam.*

[2]*Vietnam National University Ho Chi Minh City, Linh Trung Ward, Thu Duc District, Ho Chi Minh City, Vietnam.*

**Correspondence**

**Vu Cong Hoa**, Department of Engineering Mechanics, Faculty of Applied Sciences, Ho Chi Minh City University of Technology, 268 Ly Thuong Kiet Street, District 10, Ho Chi Minh City, Vietnam.

Vietnam National University Ho Chi Minh City, Linh Trung Ward, Thu Duc District, Ho Chi Minh City, Vietnam.

Email: vuconghoa@hcmut.edu.vn

**History**

- Received: 22-9-2021
- Accepted: 17-3-2022
- Published: 31-5-2022

**DOI :** 10.32508/stdjet.v4iSI2.921

Check for updates



## INTRODUCTION

As mentioned in B. Meyghani *et al.* [1], Welding was first employed by the Sumerian civilisation to join copper items. Welding's importance grew dramatically after World War I. Because all countries were barred from building ships greater than 10,000 tons per the Treaty of Versailles. Therefore, German engineers began to study the joining methods for warships and then they may be able to reduce the ship's weight by thousands of tons. Since then, the weight as a significant factor in design of ships. According to the recent news, people have been and are facing several global problems such as the greenhouse effect and reducing natural resources. So, the need for reducing fuel consumption and using environmentally friendly technologies are also increasing. As a result, a lot of research has gone into developing new joining technologies and determining their fatigue life in order to produce lightweight details.

The Welding Institute (TWI) in the United Kingdom invented friction stir welding (FSW) in 1991 [2]. It has been used to join non-ferrous metals and aluminum alloys of different thicknesses, physical, chemical and mechanical qualities [3]. FSW differs from other traditional welding procedures in that it does not melt the materials being connected. First, two sheets of material are held in place and clamped together. In the second step, the welding pin is mounted in a high-speed rotating chuck placed on the weld to heat the material by friction. Heat is generated as a result of the friction, which raises the temperature of the plates. Once the pin is fully inserted, it is pushed in the welding direction at a minor angle. An advancing side and a

**Cite this article :** Nhu D H, Hoa V C. **Analysis the influence of threaded pin profiles in friction stir welding by numerical simulation**. *Sci. Tech. Dev. J. – Engineering and Technology;* 4(SI2):SI57-SI67.

retreating side are formed as the softened and heated material flows around the pin to its backside, where it is consolidated to create a solid-state weld, thanks to forward and rotational movement of the pin and shoulder of the tool along the weld[2]. On cooling, a solid phase bond is created between the workpieces. (Figure 1).

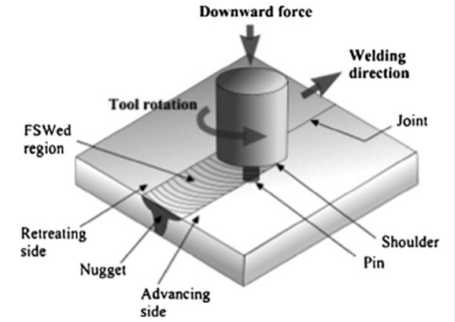


**Figure 1**: Mechanism of Friction Stir Welding[2].

There are many parameters affecting the mechanical properties of weldment in FSW such as translational speed, rotational speed, tool geometry (pin profile), thickness of the workpiece, workpiece material, welding tool material and other things. In FSW, however, the pin profile and its size are vital factors for the weld quality. Using a finite element method model, G. Buffa et al[4] studied the effect of tool tilt angle on flow of material and grain size distribution. The obtained result allows using a conical pin with pin angle of 40o speed and speed equal to 100 mm/min to get the best joint strength. K. Elangovan et al[5] investigated the impact of tool pin profile and tool shoulder diameter in AA6061 aluminum alloy by experiment. Z. Sun et al[6] studied the effects of pin thread profile on heat generation, temperature distribution and material field by a numerical model. Pin thread profile is proposed when it comes to use FSW process because material flow velocity and area of TMAZ (thermal-mechanically affected zone) for pin thread are bigger than for pin unthread. The obtained result allows using a conical pin with pin angle of $40^o$ and an advancing speed equal to 100 mm/min to get the best joint strength.

There are several simulation methods in FSW like Computational Fluid Dynamic (CFD), Arbitrary Lagrangian Eulerian (ALE) formulation and Couple Eulerian-Lagrangian modeling (CEL). M. Safari et al[7] used CEL modeling to analyze in dissimilar aluminum alloy with three pin profiles. The temperature distribution from experimental measurements and simulation modeling agreed well in this investigation. Besides that, Fadi Al-Badour[8] also researched influence on the coefficient of friction in weldment's void formation by using CEL simulation method. This study concluded that using friction coefficient lower, the void is larger. According to this author, CFD simulation has many disadvantages. First, full sticking contact conditions are commonly assumed, resulting in overestimation of weld peak temperature and tool reaction loads. The elasticity of the material was also overlooked by CFD simulations. For the ALE technique[7], it can take into consideration temperature. However, the Lagrangian elements cannot deal with the void formation so serious mesh distortion will happen in the large deformation analysis. The Eulerian elements are dependent on the volume-of-fluid approach, in which the material's Eulerian Volume Fraction is tracked as it flows through the mesh (EVF). Therefore, the Eulerian elements can deal with multiple materials and also void formations, which is an advantage.

In the current research, FSW process is simulated with CEL methods on ABAQUS software. The CEL methods has much more disadvantages than the ALE technique. This is the optimal combination between benefit of Lagrangian mesh and Eulerian mesh. This method can predict the material flow and the defect formation of weldment throughout the FSW process. The purpose of this study is to investigate the impact of pin profiles threaded cylindrical-three flats with various opening angles. In comparison to previous published research, this is a new aspect of this paper. In this paper, first, the simulated model is validated with the experimental measurements that is mentioned in study He *et al.*[2]. Then, the impacts of tool pin profile on the temperature distribution and weld defect formation are investigated. The AA 7075-T6 aluminum alloys are selected for the FSW simulation with many designed pin profiles in this study. This aluminum alloy is a exhibits super high strength alloys which has been used extensively in marine fittings, automobiles and aircraft applications and other highly stressed applications.

## METHODOLOGY

### Theoretical formula

#### *Model formulation*

Using finite element software ABAQUS analyses the whole FWS process. Model includes a deformable workpiece to be assumed elastic-plastic material and rigid stirring pin tool.

The differential equation of motion in general form is[9]:

$$\rho \underline{\ddot{u}} + c\underline{\dot{u}} + k\underline{u} = p \tag{1}$$

where $\rho$ is the density, c is the damping coefficient, k is the stiffness coefficient, p is the body force and $\underline{u}$ is the displacement vector. However, in the finite element method, equation (1) is discretized into (2):

$$M\ddot{u} + C\dot{u} + Ku = P \tag{2}$$

where M is the mass matrix, C the viscous damping matrix, K the stiffness matrix, P the vector of external forces, which include body forces, surface forces and concentrated loads acting on the system, and u, $\dot{u}$ and $\ddot{u}$ are the nodal displacement, velocity and acceleration vectors, respectively.

The nodal acceleration vector in the beginning of a time increment is obtained as:

$$\ddot{u}_i = M^{-1}\left(P - C\dot{u}_i - Ku_i\right) \tag{3}$$

where $i$ denotes the time step.

Acceleration is computed by:

$$\ddot{u}_i = \frac{\dot{u}_{i+1/2} - \dot{u}_{i-1/2}}{\left(\triangle t_{i+1} + \triangle t_i\right)/2} \tag{4}$$

from which the velocity is obtained:

$$\dot{u}_{i+1/2} = \frac{\triangle t_{i+1} + \triangle t_i}{2}\ddot{u}_i + \dot{u}_{i-1/2} \tag{5}$$

Combining equations (3) and (5) gives the final explicit expression for the velocity:

$$\dot{u}_{i+1/2} = \frac{\triangle t_{i+1} + \triangle t_i}{2} M^{-1}\left(P - C\dot{u}_i - Ku_i\right) + \dot{u}_{i-1/2} \tag{6}$$

## Thermal response

The heat generation for workpiece is written[10]:

$$\rho c_p \dot{T} = \left(kT_{,i}\right)_{,i} + \eta s_{ij}\dot{\varepsilon}_{ij}^{pl} \tag{7}$$

where $c_p$ is the specific heat capacity, $k$ the thermal conductivity, $\eta$ the fraction of plastic energy dissipation, $s_{ij}$ the deviatoric stress tensor and $\dot{\varepsilon}_{ij}^{pl}$ is the plastic strain rate tensor.

The heat source Q is calculated as follows:

$$q_{surf} = \mu p \dot{\gamma} \tag{8}$$

where $\mu$ is the friction coefficient, $p$ is the pressure and $\dot{\gamma}$ is the slip rate. The classical Coulomb's friction model is used to describe the contact behavior between the pin and the workpiece. In the present model, the friction coefficient $\mu$ is set to be 0.3 according to M. Iordache et al[3].

In the finite element method, equation (7) is discretized into (9):

$$C\dot{T} + BT = S \tag{9}$$

where $C$ is the capacity matrix, $B$ the conductivity matrix, $S$ the source vector accounting for all thermal sources $T$ and $\dot{T}$ are the nodal temperature and temperature rate vectors, respectively.

The nodal temperature rate vector at the beginning of a time increment is calculated as follow:

$$\dot{T} = C^{-1}\left(S - BT_i\right) \tag{10}$$

Similarly, formulation in mechanical response, the temperature rate yield as:

$$\dot{T}_i = \frac{T_{i+1} - T_i}{\triangle t_{i+1}} \tag{11}$$

The final expansion formula is:

$$\begin{aligned} T_{i+1} &= \triangle t_{t+1}\dot{T}_i + T_i \\ &= \triangle t_{t+1} C^{-1}\left(S - BT_i\right) + T_i \end{aligned} \tag{12}$$

## Johnson – Cook material model

Johnson Cook material model is a good selection to combine hardening because simulation of the material deformation is complicated and depends on the strain, strain rate and temperature increase[7]. This model can ensure describing these influential factors. Equation of the Johnson – cook material model is showed below:

$$\sigma_0 = \left(A + B\bar{\varepsilon}_{pl}^{n}\right)\left(1 + C\ln\frac{\dot{\bar{\varepsilon}}_{pl}}{\dot{\varepsilon}_0}\right)\left(1 - \left(\frac{T - T_{ref}}{T_{melt} - T_{ref}}\right)^{m}\right) \tag{13}$$

Where $\sigma_0$ is the flow stress, $\dot{\varepsilon}$ is the strain rate, $\overline{\varepsilon_{pl}}$ is the effective plastic strain, $\dot{\varepsilon}_{pl}$ is the effective plastic strain rate, is the normalizing strain rate (typically 1.0 $s$-1). $T$ is the temperature (in Kelvin or Celsius), $T_{ref}$ is the reference temperature (usually room temperature) and $T_{melt}$ is the melting temperature of the material. Here, $n$ is the strain hardening exponent and $m$ is the strain rate sensitivity exponent, and A, B, and C are material constants. The coefficients of the Johnson-Cook plasticity model for AA 7075-T6 and AA 6082-T6 aluminum alloys, used in this analysis, are shown in section workpiece below.

## Finite Element Modeling For Friction Stir Welding process

### Computational Domain

The computational domain includes Eulerian-type domain and Lagrangian-type domain. Eulerian domain is a rectangle with dimension of mm, respectively. The dimension of workpiece is 65x60x5 mm (Length x Width x Thickness) [2]. The Lagrangian is used to tool model.

### Tool

Weld tool has two main parts including shoulder and pin. Dimension of them is referred to M. Iordache's paper[3], which is showed in picture below (Figure 2).

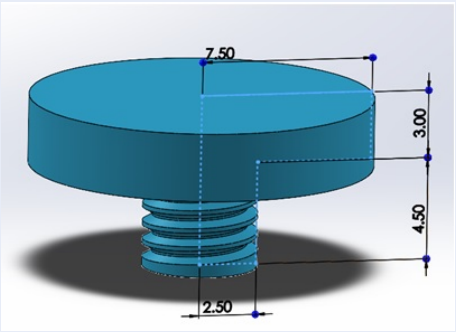


**Figure 2**: Dimension of the weld tool.

This study will investigate threaded cylindrical with three flats in pin tool. They are collectively known as threaded-three flat cylindrical pin profile. The shapes of the tool pin profiles investigated in this study are shown in Figure 3. TF0 denotes a threaded pin, whereas TF30, TF60 and TF90 denote tool pins with three flat areas, each with a different opening angle of 30°, 60°and 90°. All models are designed by SOLIDWORKS software.

Workpieces are constructed of AA 7075 – T6 and AA 6082 – T6 with a thickness of 5 mm so the tool is made of steel H13[11]. The movement process of pin is displayed in Figure 4. There are two main operations in the FSW process including rotation and movement along the weld of the tool pin at the same time. Table 1 shows properties of tool pin were used in this study.

### Workpiece

As seen in equation[13], the Johnson-Cook material was used to characterize material behavior for workpiece. The constants of this material law such as A, B, C, n and m from the equation[13] with properties of workpiece are described values from the Table 2.

**Table 1: Properties of steel H13**[12]

| | |
|---|---|
| Young's modulus | E = 210000 (MPa) |
| Poisson coefficient | $v$ = 0.3 |
| Mass density | $\rho$ = 7825 (kg/m$^3$) |
| Thermal conductivity | $k$ = 28.5 (W/m. K) |
| Specific heat | $c_P$ = 475 (J/kg. K) |

### Data input description

*Contact.* Pin-workpiece contact is a "general contact". The friction law and normal behavior is described by a "hard contact". In CEL method, this sort of interaction is linked to explicit dynamic analysis through ABAQUS software. For the static and kinetic friction coefficients, the normal practice is to utilize a value of 0.3[15].

Applying a pressure on surface of the tool simulates the force control welding condition, while fixed displacement is used for position control.

*Welding parameters introduced in the model.* The main stages in the friction welding process are:

- Step 1 *(Plunging phase)*: The tool begins to rotate and move down to plunge in the workpiece.
- Step 2 *(Dweller phase)*: Workpiece is preheating by rotation of tool at the start position.
- Step 3 *(Welding stir phase)*: While rotating, the tool moves longitudinally along the joint line.

There are several parameters in the process is showed below (Table 3).

The stages are illustrated in the diagram below (Figure 5).

*Boundary conditions.* At the start of the analysis. The entire model is provided with a fixed temperature field equal to the environmental temperature. Convection boundary conditions were assumed to exist on all of the workpiece's surfaces. Besides, displacement boundary condition is based on parameter in processing (Figure 6).

Convection boundary conditions were assumed to exist on all surfaces of the workpiece. The bottom surface in contact with backing plate has a much higher convection coefficient than the rest surface of the plate with 1000 $Wm^{-2}K^{-1}$, 10 $Wm^{-2}K^{-1}$ respectively[9].

*Meshing.* The FSW process was simulated with element sizes ranging from 0.1 mm to 0.3 mm, resulting in good modeling accuracy. However, the element size of 4 mm was utilized distant from the welding seam, whereas the size of 0.8 mm was used in the heat affected zone to save time[1]. This study uses multi-material thermally coupled element type EC3D8RT

**Table 2: Material properties and constants in Johnson – Cook model of AA 6082-T6 and AA 7075-T6** [7,13,14]

| Material | AA 6082-T6 | AA 7075-T6 |
|---|---|---|
| Properties | | |
| Young's modulus, E (MPa) | 69000 | 71700 |
| Poisson coefficient, v | 0.33 | 0.33 |
| Mass density, $\rho$ (kg/m$^3$) | 2700 | 2800 |
| Thermal conductivity, $k$ (W/m. C) | 174 | 130 |
| Specific heat, $c_P$ (J/kg. C) | 935 | 960 |
| A (MPa) | 285 | 546 |
| B (MPa) | 94 | 678 |
| C | 0.002 | 0.024 |
| m | 1.34 | 1.56 |
| n | 0.41 | 0.71 |
| $\dot{\varepsilon}$ | 1 | 1 |
| $T_{melt}$ $(C)$ | 588 | 635 |
| $T_{ref}$ $(C)$ | 25 | 20 |

**Table 3: Parameter in process using in this study**

| | Velocity (mm/s) | Rotational speed (RPM) | Time (s) |
|---|---|---|---|
| Step 1 | 5.5 | 1200 | 1 |
| Step 2 [16] | 0 | 1200 | 0.1 |
| Step 3 | 3 | 1200 | 16 |

for Eulerian elements. The number of tetra elements are used for tool pins, while 18720 hex elements for workpiece. (See Figure 7).

### *Coupled Eulerian – Lagrangian method*

Through contact interaction, the Eulerian body is linked to the Lagrangian. The welding tool is assigned Lagrangian reference model, whereas the workpieces are used the Eulerian reference model. Material points are connected to the Lagrangian mesh. The mesh will deform if the material deforms. The Eulerian, on the other hand, is utilized as a foundation grid. As the material deforms (or flows) within the mesh, the mesh remains unchanged (Figure 8 & Figure 9).

Eulerian analyses work well in situations where there is a lot of deformation, such as fluid flow. In these circumstances, Lagrangian elements become very deformed and decrease accurate. The materials become viscous throughout the welding process, and this condition may be accurately characterized using the Eulerian analysis. The volume of fluid method is used in the Eulerian methodology in ABAQUS/ Explicit. The Eulerian volume fraction (EVF) within each element is determined using this method [3]. By definition, the EVF is equal to 1 if the material completely fills an element, otherwise the EVF is equal to 0 [17]. (See Figure 9)

The volume fraction tool in the CEL technique has the benefit that it does not require meshing of the workpieces; only meshing Eulerian domain is necessary.

## RESULTS AND DISCUSSIONS

### Comparison of temperature distribution in FEM model and available experimental model.

The temperature values produced by FE simulation are compared to experimental values provided in the study of M. Iordache to validate the FE model [3]. Table IV gives information about temperature of weld in experiment obtained from line chart by Web Plot Digitizer software. Coordinate 0 assumed is the position in the middle of the weld.

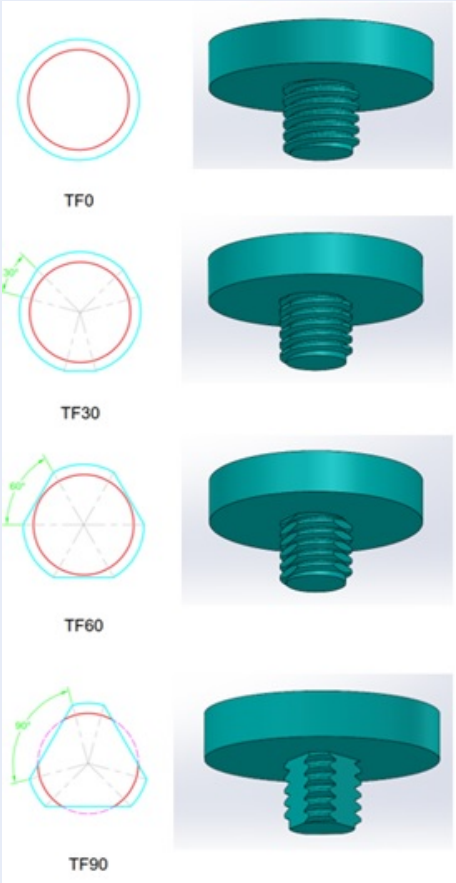


**Figure 3**: Cross section of tool pin profiles to be used in the present study.

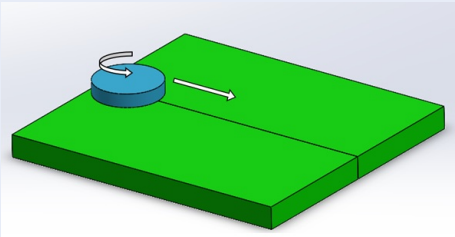

**Figure 4**: FSW process rotation and movement direction.

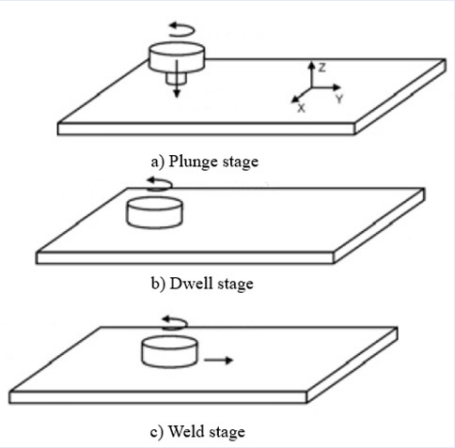


**Figure 5**: The three steps of FSW simulated in this present research

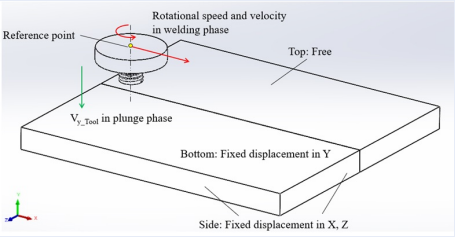


**Figure 6**: Displacement boundary conditions of model in ABAQUS software

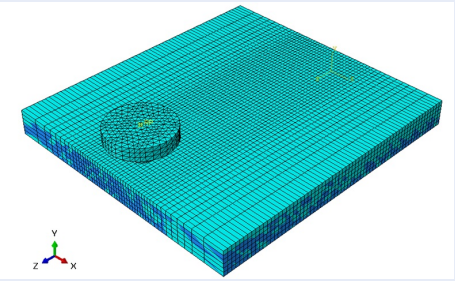

**Figure 7**: Assembly and mesh in model.

Figure 10 describes the temperature distribution fields of model FE in this study. Behavior of this FEM model is slightly similar to experimental one, for instance, the area under the shoulder has the highest temperature. This phenomenon is caused by friction between pin tool and workpiece in addition to axial force of shoulder. Temperatures on the retreating side (left side) and advancing side (right side) are almost symmetrical. However, the temp on retreating side is

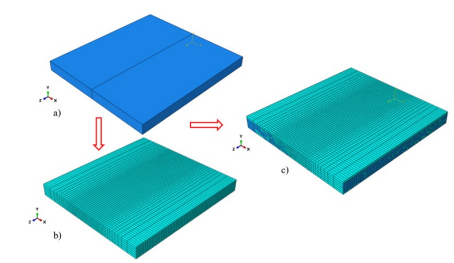

**Figure 8**: Coupled Eulerian-Lagrangian model in this study a) Eulerian body, b) Lagrangian body, c) Coupled Eulerian - Lagrangian.

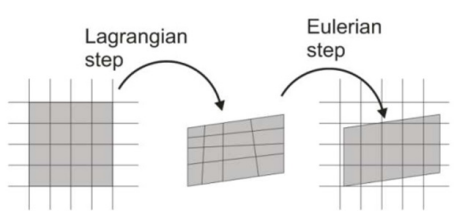


**Figure 9**: Split operator for the CEL formulation [18].

**Table 4: Temperature is measured in experiment [3]**

| Coordinate (mm) | Temperature ($^o$C) |
|---|---|
| -20 | 296.72 |
| -15 | 336.06 |
| -10 | 363.44 |
| 0 | Not measure |
| 10 | 393.44 |
| 15 | 342.62 |
| 20 | 307.38 |

about 10$^o$C - 20°C higher than on the other side. This temperature distribution characteristics are similar to those shown by H. Aghajani Derazkola [19] or H. Su [20], as well as other references. Besides that, this model can illustrate a small part of material which is got out of workpiece due to stirring process. M. Safira [7] also conducted this simulation method and obtained the same result.

Figure 11 compares temp along cross-section weldment between the results predicted in this study and the data measured in experiments. It is observed that the simulated peak temperatures are slightly lower than the experimental ones with an average error about of 14%. There are several reasons why it has this difference such as the thermal properties of material, parameters in practical process, assumption of frictional coefficient and the heat transfer coefficient. M. Safira [7] adjusted convection coefficient, radiation coefficient and ambient temperature to decrease the temperature error between experimental and simulation model results. In addition, the measurement error of thermal coupled experiment may be influence on the accuracy of this results. Although there is a difference between the simulated and measured temperatures, they are generally in good agreement.

**Figure 10**: Temperature distributions in workpiece by ABAQUS software.

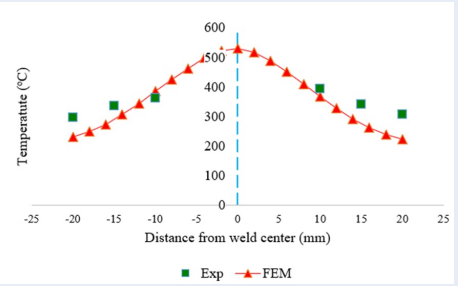


**Figure 11**: Temperature distributions along cross-section in FSW weldment after dwelling stage.

## Effects of combing threaded and three-flat in pin profile for AA7075-T6 aluminum alloys

### *Temperature distribution fields*

Figure 12 gives information about temperature distribution for four pin profiles (TF0, TF30, TF60, TF90) at the same section and welding phase. It is obviously shown that the stirring zone temperature of TF60 and TF90 seems slightly higher than TF0 and TF30, as well as its width. In addition, with the large triflat faces in TF90 leads to the ability of mixing up material strongly. This can allow the formation of quality welds, but according to Abhishek Ajri [21] weld defects can be caused by large temperature differences

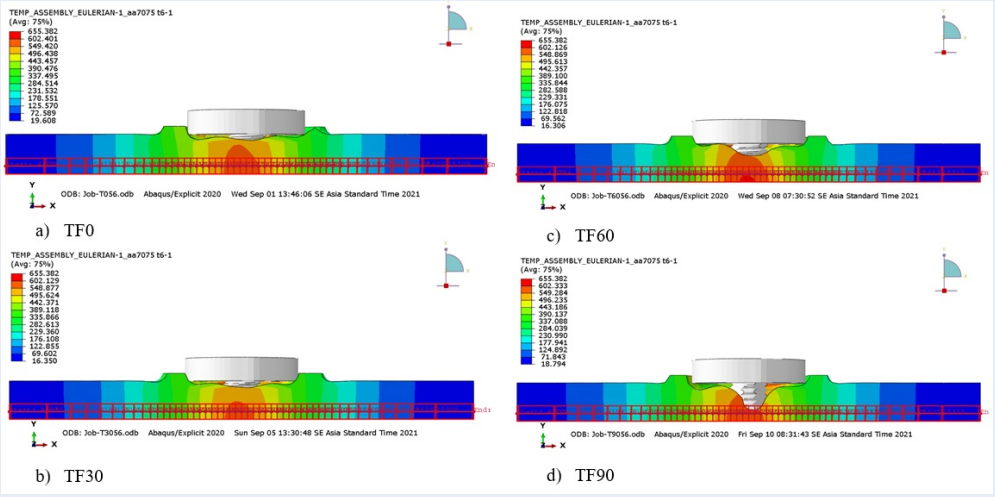


**Figure 12**: Temperature distribution field for combining between threaded and three-flat of pins.

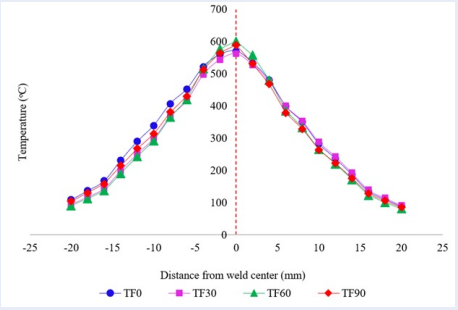


**Figure 13**: Temperature comparison line chart of four pin profiles.

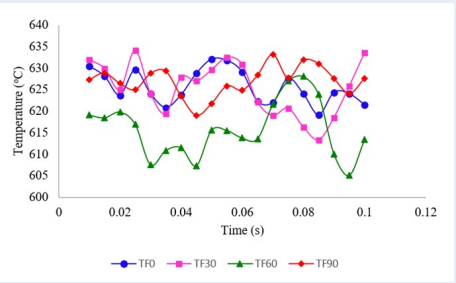


**Figure 14**: The process of heating and softening the material in dweller phase.

on both sides of the weld. A line chart (Figure 13) illustrates temperature filed for various pin profiles in this study. Overall, TF30 and TF60 has less different temperature between the joint of FSW process around $20^oC$ – $30^oC$ than TF0 and TF90. The excessive material stirring of TF90 causes the large non-uniform heat transfer. It is noticed that the peak temp at TF60 is highest with approximately $600^oC$, so it can make soften weldment zone better and it leads to higher weld strength [22].

In Figure 14 heat generation and softening in material are described by oscillation of temperature in dweller phase before welding.

Obviously, there is a dramatic fluctuation of temperature for TF60 with the highest being $628^oC$ and the lowest being $605^oC$. Likewise, $633^oC$ and $613^oC$ are the highest and lowest number respectively for TF30. Meanwhile, T90 and T0 are oscillate slightly which can make the process of heating and softening weldment in dweller phase better.

## *Void formation*

As mentioned above theory, Coupled Eulerian – Lagragian methods is used to investigate void formation by Eulerian Volume Fraction option in the ABAQUS software. Figure 15 shows the effects of pin profile in this research with the red region represents a void entirely (EVF_VOID = 1) and the blue region represents full material (EVF_VOID = 0). As it is seen in Figure 15 – T90, there is a big void on the right side proving that its ability stirring the material is not good. Overall, all three of pin profiles (TF0, TF30, T60) do not create many voids, but TF60 is a good profile since it stirs material smoothly better (no red region at advancing side and retreating side).

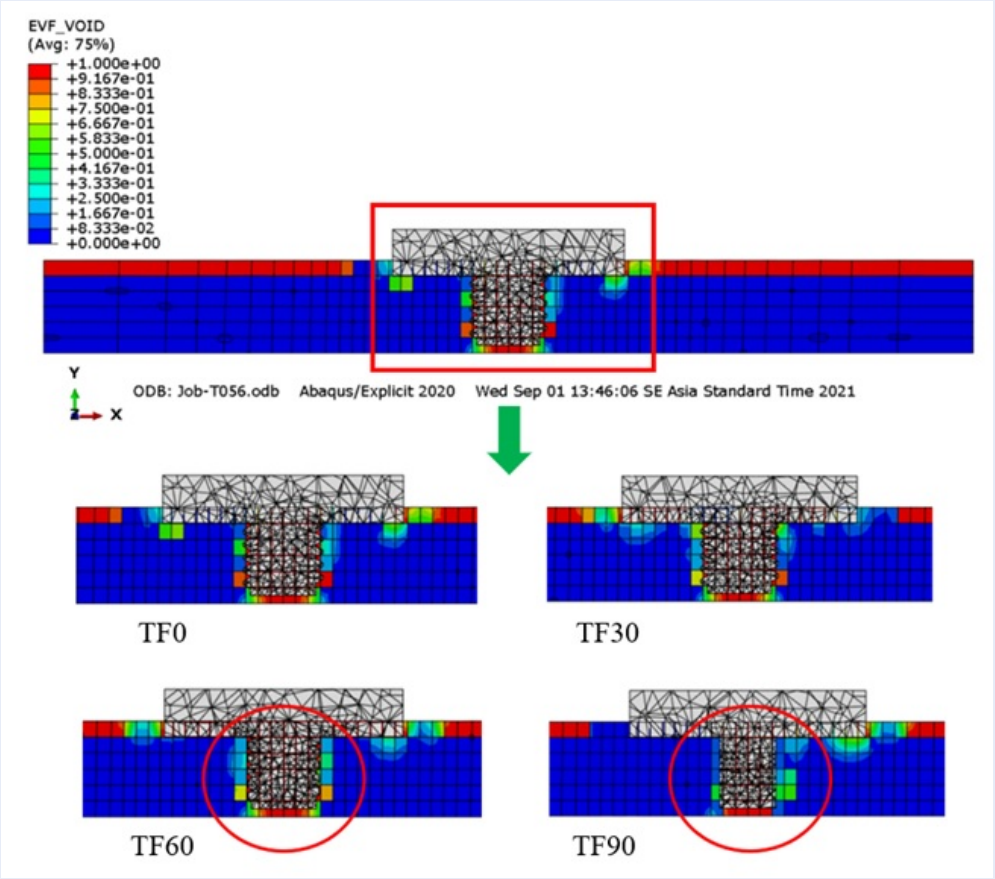


**Figure 15**: A comparison of the void formation for four pin profiles.

## CONCLUSION

In this work, the numerical simulation of four pin profiles in friction stir welding with the combination between threaded and three-flat (three-flat) was investigated. A 3D Coupled Eulerian-Lagrangian (CEL) model was used in the ABAQUS software. The influence of pin profiles was evaluated through the temperature distribution and void information. The following are the results of the research presented:

1. There is a difference between the temperature distribution was measured from numerical simulations and experimental model with average error 14%. Yet, this difference can be explained by a variety of objective factors. As a result, this model managed to use in this study.
2. The ability to mix the material of the TF60 welding pin is stronger than that of the common threaded welding pin, but the material is not stirred too strongly as in the case of 90 opening angle causing large weld defects and the temperature difference of two aluminum alloy plates. Therefore, temperature distribution in TF60 is the most symmetrical in the welding phase.
3. The heat generation and softening material in dweller phase has a dramatic fluctuation for TF60 and TF30.
4. EVF option (Eulerian Volume Fraction) can evaluate and analyze void formation pretty well. As a result, pin profile T60 stirs material better than other profiles in this study.
5. However, this FE model of the FSW process has a number of drawbacks. It is difficult to describe entirely weld behavior because this FSW is a complex phenomenon consist of mechanical and thermal processes. Therefore, the next task is to make an experimental model for this study to adjust many suitable parameters in this numerical simulation such as radiation, convection and friction coefficient.

## ABBREVIATION

FSW: Friction stir welding

FEMs: Finite Element Methods
TWI: The Welding Institute
CFD: Computational Fluid Dynamic
ALE: Arbitrary Lagrangian Eulerian
CEL: Couple Eulerian-Lagrangian

## ACKNOWLEDGEMENT

We acknowledge the support of time and facilities from Ho Chi Minh City University of Technology (HCMUT), VNU-HCM for this study.

## CONFLICT OF INTEREST

Group of authors declare that this manuscript is original, has not been published before and there is no conflict of interest in publishing the paper.

## AUTHORS' CONTRIBUTION

Do Huynh Nhu is work as the chief developer of the method of research, gathering data and the manuscript editor.

Vu Cong Hoa is the supervisor, contributes ideas for the proposed method and also takes part in checking the data and simulation results and manuscript.

## REFERENCES

1. Meyghani B, Awang M, Emamian SS, Mohd Nor MK, Pedapati SR. A Comparison of Different Finite Element Methods in the Thermal Analysis of Friction Stir Welding (FSW). Metals. 2017;7(10);Available from: https://doi.org/10.3390/met7100450.
2. He X, Gu F, Ball A. A review of numerical analysis of friction stir welding. Progress in Materials Science. 2014;65:1-66;Available from: https://doi.org/10.1016/j.pmatsci.2014.03.003.
3. Iordache M, Badulescu C, Iacomi D, Nitu E, Ciuca C. Numerical Simulation of the Friction Stir Welding Process Using Coupled Eulerian Lagrangian Method. Materials Science and Engineering. 2016;145;Available from: https://doi.org/10.1088/1757-899X/145/2/022017.
4. Buffa G, Hua J, Shivpuri R, Fratini L. Design of the friction stir welding tool using the continuum based FEM model. Materials Science and Engineering: A. 2006;419(1-2):381-8;Available from: https://doi.org/10.1016/j.msea.2005.09.041.
5. Elangovan K, Balasubramanian V. Influences of tool pin profile and tool shoulder diameter on the formation of friction stir processing zone in AA6061 aluminium alloy. Materials & Design. 2008;29(2):362-73;Available from: https://doi.org/10.1016/j.matdes.2007.01.030.
6. Sun Z, Wu CS. A numerical model of pin thread effect on material flow and heat generation in shear layer during friction stir welding. Journal of Manufacturing Processes. 2018;36:10-21;Available from: https://doi.org/10.1016/j.jmapro.2018.09.021.
7. Safari M, Joudaki J. Coupled Eulerian-Lagrangian (CEL) Modeling of Material Flow in Dissimilar Friction Stir Welding of Aluminum Alloys. Iranian Journal of Materials Forming 2019;6:10-9;.
8. Al-Badour F, Merah N, Shuaib A, Bazoune A. Coupled Eulerian Lagrangian finite element modeling of friction stir welding processes. Journal of Materials Processing Technology. 2013;213(8):1433-9;Available from: https://doi.org/10.1016/j.jmatprotec.2013.02.014.
9. Schmidt H, Hattel J. A local model for the thermomechanical conditions in friction stir welding. Modelling and Simulation in Materials Science and Engineering. 2005;13(1):77-93;Available from: https://doi.org/10.1088/0965-0393/13/1/006.
10. En-zhi G, Xing-xing Z, Chun-zhong L, Zong-yi M. Numerical simulations on material flow behaviors in whole process of friction stir welding. Transactions of Nonferrous Metals Society of China. 2018;28(11):2324-34;Available from: https://doi.org/10.1016/S1003-6326(18)64877-0.
11. R. R, A. D, H. BHKD, T. D. Review: friction stir welding tools. Science and Technology of Welding and Joining. 2013;16(4):325-42;Available from: https://doi.org/10.1179/1362171811Y.0000000023.
12. M. G, G. A, B. P, M. OJ, F. YC, A. CB, et al. Computational Analysis of Material Flow During Friction Stir Welding of AA5059 Aluminum Alloys. Journal of Materials Engineering and Performance. 2011;21(9):1824-40;Available from: https://doi.org/10.1007/s11665-011-0069-z.
13. Birsan D, Scutelnicu E, Visan D. Behaviour Simulation of Aluminium Alloy 6082-T6 during Friction Stir Welding and Tungsten Inert Gas Welding. Manufacturing Engineering.31;.
14. 7075-T6 PoA. 2016;Available from: http://asm.matweb.com/search/SpecificMaterial.asp?bassnum=MA7075T6.
15. Grujicic M, Snipes JS, Ramaswami S, Galgalikar R, Yen CF, Cheeseman BA. Computational analysis of the intermetallic formation during the dissimilar metal aluminum-to-steel friction stir welding process. Materials: Design and Applications. 2017;233(6):1080-100;Available from: https://doi.org/10.1177/1464420716673670.
16. Hamilton R, MacKenzie D, Li H. Multi-physics simulation of friction stir welding process. Engineering Computations. 2010;27(8):967-85;Available from: https://doi.org/10.1108/02644401011082980.
17. Simulia. ABAQUS analysis user's manual. 2014;.
18. Skrzat A. Application of Coupled Eulerian-Lagrangian approach in metal forming simulations. Mechanika. 2012;84:4-12;Available from: https://doi.org/10.7862/rm.2012.9.
19. Aghajani Derazkola H, Khodabakhshi F. Intermetallic compounds (IMCs) formation during dissimilar friction-stir welding of AA5005 aluminum alloy to St-52 steel: numerical modeling and experimental study. Advanced Manufacturing Technology. 2018;100(9-12):2401-22;Available from: https://doi.org/10.1007/s00170-018-2879-8.
20. Su H, Wu CS, Pittner A, Rethmeier M. Thermal energy generation and distribution in friction stir welding of aluminum alloys. Energy. 2014;77:720-31;Available from: https://doi.org/10.1016/j.energy.2014.09.045.
21. Ajri A, Rohatgi N, Shin YC. Analysis of defect formation mechanisms and their effects on weld strength during friction stir welding of Al 6061-T6 via experiments and finite element modeling. The International Journal of Advanced Manufacturing Technology. 2020;107(11-12):4621-35;Available from: https://doi.org/10.1007/s00170-020-05353-3.
22. Kumar TP. Influence of Tool Geometry in Friction Stir Welding on Material Flow Pattern. International Journal of Current Engineering and Technology. 2013;2(2):230-5;Available from: https://doi.org/10.14741/ijcet/spl.2.2014.41.

*Tạp chí Phát triển Khoa học và Công nghệ – Engineering and Technology, 4(SI2):SI57-SI67*

Open Access Full Text Article

*Bài nghiên cứu*

# Phân tích ảnh hưởng của biên dạng chốt ren trong hàn ma sát khuấy bằng mô phỏng số

**Đỗ Huỳnh Như[1,2], Vũ Công Hòa[1,2,*]**

Use your smartphone to scan this QR code and download this article

**TÓM TẮT**

Ngày nay, ngành công nghiệp hàn có những đóng góp không nhỏ trong hầu hết các lĩnh vực sản xuất nhằm đáp ứng nhu cầu đời sống của con người. Tuy nhiên, phương pháp hàn truyền thống có các nhược điểm như: năng lượng tiêu hao lớn, sản sinh ra nhiều khí độc hại cho môi trường và sức khỏe công nhân. Vì vậy, phương pháp hàn ma sát khuấy ra đời từ sự nghiên cứu của các nhà khoa học để giải quyết các nhược điểm trên. Mặt khác, nó còn thích hợp để ghép nối các hợp kim nhôm và các kim loại màu có nhiệt độ nóng chảy thấp với nhau. Công nghệ hàn xanh này không ngừng được nghiên cứu để nâng cao chất lượng mối hàn thông qua hai mô hình nghiên cứu chính là mô hình thực nghiệm và mô phỏng số. Kết quả thực nghiệm sẽ cung cấp các tính chất cơ học cơ bản của vật liệu tại mối hàn và các thông số tối ưu hóa quá trình hàn. Đây sẽ là cơ sở để thiết lập mô hình mô phỏng số quá trình này gần với thực tế nhất, dựa trên mô hình toán học và nguyên lí làm việc của nó, từ đó giúp dự đoán chất lượng mối hàn thông qua dự đoán sự hình thành khuyết tật, phân bố nhiệt độ trong mối hàn với sự thay đổi các thông số quá trình như vận tốc di chuyển, vận tốc quay và thời gian trong từng giải đoạn hàn. Trong nghiên cứu này, ảnh hưởng của biên dạng chốt ren đến chất lượng mối hàn của hợp kim nhôm 7075 -T6 trong quá trình hàn khuấy ma sát đã được khảo sát bằng mô hình mô phỏng số thông qua phần mềm ABAQUS để đề xuất một biên dạng chốt mới mang lại chất lượng mối hàn tốt hơn. Để tăng độ tin cậy của phương pháp nghiên cứu này, kết quả mô phỏng số về phân bố nhiệt độ được so sánh với kết quả thực nghiệm thu được từ một bài báo khoa học nước ngoài với sai số trung bình là 14%. Các cấu hình chốt ren được thiết kế kết hợp với ba mặt cắt có góc mở khác nhau có tên là TF0, TF30, TF60 và TF90. Phương pháp Coupled Eulerian-Lagrangian được áp dụng cho mô hình này, trong đó dụng cụ hàn là miền Lagrangian và phôi là miền Eulerian. Do biến dạng vật liệu trong quá trình hàn khuấy ma sát lớn và liên quan đến nhiệt độ nên mô hình vật liệu Johnson-Cook được sử dụng cho phôi. Kết quả của nghiên cứu này cho thấy một cấu hình chốt mới có tên là TF60, nó cho chất lượng mối hàn tốt nhất trong bốn loại chốt hàn được khảo sát trong nghiên cứu này thông qua việc đánh giá sự phân bố nhiệt độ và dự đoán sự hình thành khuyết tật mối hàn.

**Từ khoá:** Hàn ma sát khuấy, biên dạng chốt, mô phỏng số, Coupled Eulerian-Lagrangian, mô hình Johnson – Cook model

[1]*Bộ môn Cơ Kỹ thuật, Khoa Khoa học Ứng dụng, Trường Đại học Bách khoa, 268 Lý Thường Kiệt, Quận 10, Thành phố Hồ Chí Minh, Việt Nam*

[2]*Đại học Quốc gia Thành phố Hồ Chí Minh, Thành phố Hồ Chí Minh, Việt Nam*

**Liên hệ**

**Vũ Công Hòa**, Bộ môn Cơ Kỹ thuật, Khoa Khoa học Ứng dụng, Trường Đại học Bách khoa, 268 Lý Thường Kiệt, Quận 10, Thành phố Hồ Chí Minh, Việt Nam

Đại học Quốc gia Thành phố Hồ Chí Minh, Thành phố Hồ Chí Minh, Việt Nam

Email: vuconghoa@hcmut.edu.vn

**Lịch sử**

- Ngày nhận: 22-9-2021
- Ngày chấp nhận: 17-3-2022
- Ngày đăng: 31-5-2022

**DOI : 10.32508/stdjet.v4iSI2.921**

Check for updates



VNUHCM PRESS
25 years of scholarly publishing
1997-2022

**Trích dẫn bài báo này:** Như D H, Hòa V C. **Phân tích ảnh hưởng của biên dạng chốt ren trong hàn ma sát khuấy bằng mô phỏng số**. *Sci. Tech. Dev. J. - Eng. Tech.;* 4(SI2):SI57-SI67.